Diffusion and Conformation of Peptide-Functionalized Polyphenylene Dendrimers Studied by Fluorescence Correlation and ^{13}C NMR Spectroscopy

K. Koynov, G. Mihov, M. Mondeshki, C. Moon, H. W. Spiess,* K. Müllen, and H-J. Butt

Max-Planck-Institut für Polymerforschung, D-55021 Mainz, Germany

G. Floudas*

University of Ioannina, Department of Physics, P.O. Box 1186, 451 10 Ioannina, Greece and Foundation for Research and Technology-Hellas (FORTH), Biomedical Research Institute (BRI)

Received March 7, 2007

We report on the combined use of fluorescence correlation spectroscopy (FCS) and ^1H and ^{13}C NMR spectroscopy to detect the *size* and *type* of peptide secondary structures in a series of poly-Z-L-lysine functionalized polyphenylene dendrimers bearing the fluorescent perylenediimide core in solution. In dilute solution, the size of the molecule as detected from FCS and ^1H NMR diffusion measurements matches nicely. We show that FCS is a sensitive probe of the core size as well as of the change in the peptide secondary structure. However, FCS is less sensitive to functionality. A change in the peptide secondary conformation from β-sheets to α-helices detected by ^{13}C NMR spectroscopy gives rise to a steep increase in the hydrodynamic radii for number of residues $n \geq 16$. Nevertheless, helices are objects of low persistence.

I. Introduction

Dendrimers are macromolecules that combine high structural precision with a compact molecular structure and high end-group functionality.[1] These unique structural features of dendrimers have been used recently in biomedical applications both for the development of advanced diagnostic tools as well as for therapeutic purposes.[2,3] With respect to the latter, dendrimers have been employed as carriers for controlled drug delivery, in gene transfection, in boron neutron-capture therapy, and as novel antimicrobial peptides.[2] Central to this problem is the design of multiple antigen peptides (MAP), i.e., the attachment of several polypeptides to nanoparticles to form synthetic molecules of high immunological value.[4−6] The use of synthetic branched oligolysine carriers for attaching multiple copies of antigens has been explored.[2−6] However, these carriers do not exhibit well-defined spatial conformations, and that could have an unfavorable effect on the presentation of antigens on the immune system.[3] On the other hand, dendrimers bearing polypeptides with predetermined secondary structures are useful for the design of MAPs.

Recently, the synthesis of polyphenylene dendrimers (PPDs) as unique shape-persistent multifunctional molecules has been reported[1] as well as the synthesis of peptide-functionalized PPDs that could be used as improved MAPs.[7] Their properties in the solid state have been examined by X-rays and NMR, and a striking dependence of the polyphenylene self-assembly driven by the polylysine length was found.[8] Moreover, it was shown that poly-L-lysines can adopt a different secondary structure as compared to their linear analogues when attached to polyphenylene cores. Here we exploit that the PPDs can be synthesized using the strongly fluorescent perylenediimide core that offers the possibility of optical detection. Then, fluorescence correlation spectroscopy (FCS),[9] which is capable of investigating the dynamics of single molecules in solution, can be employed for the characterization of the peptide-functionalized PPDs. The method is based on detecting the fluctuations of the fluorescent light intensity in a small observation volume, usually formed by the focus of a confocal microscope. Due to minimal requirements on sample amounts and its high sensitivity, FCS has found widespread applications, probing quantities such as diffusive behavior,[10,11] reaction kinetics,[12] and intracellular particle concentrations.[13]

Here we report on combining FCS and ^{13}C NMR spectroscopy to detect the *size* and *type* of peptide secondary structures in poly-Z-L-lysine functionalized PPDs bearing the fluorescent perylenediimide core in DMSO solutions. The reason for using this solvent instead of a more biologically relevant one is the solubility of the compounds. For this purpose we employ polyphenylene cores of the first and second generation substituted with a series of poly-Z-L-lysines with degrees of polymerization in the range from 14 to 84 of the $G_gF_fN_n$ type, where G, F, and N stand, respectively, for generation, lysine functionality, and peptide degree of polymerization with values in the range of $1 \leq g \leq 2$, $4 \leq f \leq 16$, and $14 \leq n \leq 84$. We study their hydrodynamic properties as a function of the core size, functionality, and polypeptide length. In parallel, we employ diffusion-ordered NMR spectroscopy (DOSY) to compare with the FCS size in dilute DMSO solutions and ^{13}C NMR to investigate the polypeptide secondary structure. DOSY has the advantage that it can yield diffusion coefficients for all ^1H resonances in the NMR spectrum, but measurements are limited to relatively concentrated solutions because of the lower sensitivity of the method.[14] In this respect, FCS is superior in that it is highly sensitive toward very dilute solutions, but NMR allows us to study the diffusion of the solvent as well. We show that FCS is a sensitive probe of the core size and of the change in the peptide secondary structure but less sensitive to functionality. These results could be helpful in the design of efficient MAPs.

* Corresponding authors. E-mail: spiess@mpip-mainz.mpg.de (H.W.S.); gfloudas@cc.uoi.gr (G.F.).

10.1021/bm0702760 CCC: $37.00
Published on Web 04/19/2007

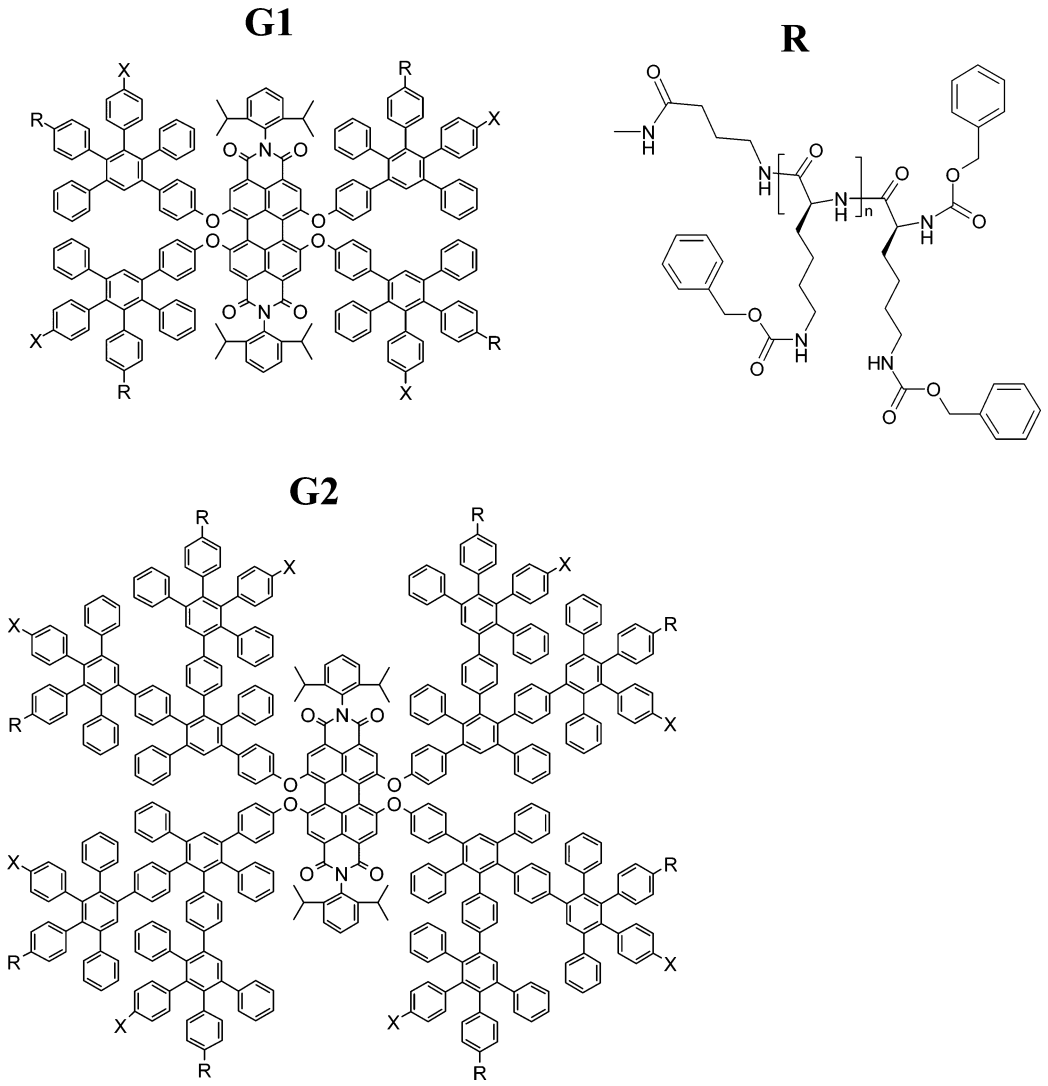

Figure 1. Polyphenylene scaffold of dendrimers of the first (top) and second (bottom) generation. X is either H or R. The repeat unit of the protected lysine (R) is also shown.

II. Experimental Section

Samples. Polyphenylene dendrimers (PPDs) are highly branched, monodisperse macromolecules consisting exclusively of benzene rings which impart shape persistence as well as chemical and photochemical inertness.[1] In previous work[7] it has been demonstrated that by applying either a priori or posteriori functionalization one can introduce a defined number of functional groups at the center, within the dendritic branches and/or at the periphery of the dendrimer. In addition, the PPDs can be synthesized not only as all-carbon structures but also using strongly fluorescent perylene dyes as a core. This approach requires both a suppression of chromophore−chromophore interactions by dendronization and a controlled multifunctionalization of the chromophore.[15] Recently, a dendrimer with a perylenediimide core bearing poly(ethylene oxide) chains has been applied as a support for metallocene catalysts in polyolefin synthesis. The fluorescent core enabled a detailed study on the fragmentation of the catalyst particles inside the polyolefin.[16]

The detailed synthesis of the poly-Z-L-lysine functionalized PPDs, described here, is published elsewere.[7] Briefly, the poly-ϵ-benzyloxicarbonyl-L-lysine chains were grafted directly from the surface of first- and second-generation, amino-functionalized PPDs consisting of pentaphenylbenzene units and a rigid perylenediimide core. The grafting of the protected polypeptides from the surface of the dendrimer was achieved via ring-opening polymerization of ϵ-benzyloxicarbonyl-L-lysine *N*-carboxy-anhydride (Lys(Z)-NCA). This reaction scheme permits control of the polypeptide length via the amount of the Lys(Z)-NCA added to the reaction. The resulting starlike polylysines possess different numbers of poly-ϵ-benzyloxicarbonyl-L-lysine chains of variable length as shown in Figure 1. The molecular characteristics of the PPDs of the $G_gF_fN_n$ type are given in Table 1. The emissive core of the dendrimer facilitates a study of the diffusion behavior of conjugates by FCS.

Fluorescence Correlation Spectroscopy (FCS). We used a commercial FCS setup (Carl Zeiss, Jena, Germany) consisting of the module ConfoCor 2 and an inverted microscope model Axiovert 200. For our experiments we employed a Zeiss plan neofluar 40×/0.9 multi-immersion objective. We used glycerol as immersion liquid because its refractive index is close to that of DMSO. The chromophores were excited with a He−Ne laser at 543 nm, and the emission was collected after filtering with a LP560 long-pass filter. For detection, an avalanche photodiode enabling single-photon counting was used. The eight-well, polystyrene chambered cover-glass (Lab-Tek, Nalge Nunc International) was used for the sample cells for the DMSO solutions of the polyphenylene cores and the poly-Z-L-lysine functionalized PPDs. These cells had bottom slides with high optical quality surface and thickness of 0.17 mm. Solutions with typical concentration of about 10^{-7} M were used in all experiments. While such concentrations are a bit too high for optimal contrast in the measured autocorrelation curves, they were necessary in order to compensate for the relatively weak fluorescence efficiency of the PPDs. For each solution, 20 measurements with total duration of 10 min were performed. The obtained autocorrelation curves

Table 1. Molecular Characteristics and Hydrodynamic Radii of the Poly-Z-L-lysine Substituted Polyphenylene Dendrimers

sample	generation	X	$n_{Lys,UV}$[a]	$n_{Lys,GPC}$[b]	M_w/M_n[c]	R_H (nm)[d]
$G_1F_4N_{14}$	1	H	9	14	1.11	2.5
$G_1F_4N_{54}$	1	H	50	54	1.16	6.2
$G_1F_4N_{84}$	1	H	85	84	1.15	7.2
$G_1F_8N_{12}$	1	R	9	12	1.09	2.9
$G_1F_8N_{60}$	1	R	68	60	1.08	7
$G_1F_8N_{74}$	1	R	76	74	1.10	
$G_2F_8N_9$	2	H	6	9	1.17	2.2
$G_2F_8N_{22}$	2	H	28	22	1.42	
$G_2F_8N_{37}$	2	H	41	37	1.27	5.7
$G_2F_{16}N_{16}$	2	R	14	16	1.26	4.6
$G_2F_{16}N_{58}$	2	R	41	58	1.50	
$G_2F_{16}N_{68}$	2	R	89	68	1.42	7.6
G_1	1					1.1
G_2	2					1.7

[a] Number of peptide residues per chain obtained from UV. [b] Number of peptide residues per chain obtained from GPC. [c] Polydispersity of the peptide−dendrimer conjugates calculated from gel permeation chromatography, obtained in DMF against polystyrene standards. [d] Obtained from the Stokes−Einstein (SE) equation.

were fitted with the so-called biophysical model function as described later, in order to determine the characteristic diffusion times of the labeled PPDs. Furthermore, fluorescently labeled silica nanoparticles (Kisker, Germany) with hydrodynamic radius in DMSO of about 42 nm, as measured with dynamic light scattering (DLS), were used for calibration of the confocal observation volume.

Dynamic Light Scattering (DLS). For the DLS experiment, we used a commercial instrument (ALV-5000 GmbH/Langen, Germany), and an ALV-5000E correlator was employed to measure the correlation function of scattered light. The measurements were carried out in the angular range of $30° < \theta < 150°$ at room temperature. A Kr-ion laser was used as the light source (wavelength $\lambda = 647.1$ nm). A cylindrical cell having an i.d. of 18 mm was placed in a thermostated bath. All solutions were filtered directly into the cylindrical cell through 0.45 μm membrane filters (Millipore).

Diffusion-ordered NMR spectroscopy (DOSY) experiments[17] were performed at 318 K in DMSO-d_6 at concentrations of 10^{-3} and about 10^{-7} M, corresponding to the ^{13}C NMR and FCS experiments, respectively. A Bruker AVANCE 700 NMR spectrometer equipped with dual *z*-gradient probe head with 55.2 G cm^{-1} gradient strength was used. Stimulated-echo sequence incorporating bipolar gradient pulses and a longitudinal eddy current delay (BPP-LED) was employed. The gradient strength was incremented in 32 steps from 2% up to 95% of the maximum gradient strength. Typical diffusion time and diffusion gradient pulse were 200 and 2.5 ms, respectively. The DOSY diffusion coefficients for the dilute solutions can be found in the Supporting Information.

^{13}C Solution-State NMR. The compounds investigated are insoluble in water. Thus, prior to the NMR experiments DMSO solutions of the respective dendrimers with a concentration of 10^{-3} M were prepared. In some cases, initial heating to 50 °C was needed to enhance solubility. The NMR measurements were conducted on a Bruker AMX 500 spectrometer at ambient temperature. For all experiments 100 k scans were recorded using a composite pulse decoupling scheme and a recycle delay of 3 s. The spectra were baseline corrected, and a broadening of 10 Hz was applied. The ^{13}C chemical shifts are referenced to external TMS.

III. Results and Discussion

FCS is based on detecting and analyzing the fluorescence light emitted by chromophores diffusing through a small and fixed observation volume element *V*, usually formed by a laser focused into the sample of interest using confocal optics. From the measured temporal fluctuations of the fluorescence intensity, $\delta I(t)$, an autocorrelation function

$$G(\tau) = 1 + \frac{\langle \delta I(t)\, \delta I(t+\tau)\rangle}{\langle I(t)\rangle^2} \tag{1}$$

corresponding to the probability that a chromophore inside the volume *V* at time *t* will still be inside at time $t + \tau$ can be evaluated. Subsequently, this measured autocorrelation function shows a decay related to the free 3D diffusion and can be fitted to the so-called biophysical model function[18]

$$G(\tau) = 1 + \frac{1}{N^*}\left(1 + \frac{\tau}{\tau_D}\right)^{-1}\left(1 + \frac{\tau}{S^2\tau_D}\right)^{-1/2} \tag{2}$$

where N^* is the average number of fluorescent molecules in the observation volume *V*, τ_D is the lateral diffusion time that a molecule stays in this volume, and $S = z_0/r_0$ is the ratio of axial to radial dimensions of *V* ($S \approx 10$ in our experiment). For a molecule with hydrodynamic radius R_H much smaller than the detection volume ($R_H \ll r_0$), the diffusion coefficient *D* can be determined from the diffusion time τ_D, as $D = r_0^2/4\tau_D$. Subsequently, the hydrodynamic radius of spherical molecules can be calculated from the Stokes−Einstein (SE) relation:

$$R_H = \frac{k_B T}{6\pi\eta D} \tag{3}$$

where k_B is Boltzmann's constant, *T* is the temperature, and η is the viscosity of the solution. For nonspherical molecules eq 3 does not apply. If the molecule can be approximated as a rod or as an ellipsoid the diffusion coefficient can be calculated from[19]

$$D_{Rod} = \frac{k_B T}{3\pi\eta L}\ln(x + u) \tag{4}$$

where *x* is the ratio of the molecular length to its diameter and $u = 0.312 + 0.565/x + 0.1/x^2$.

In Figure 2, top, the experimentally obtained correlation functions and their fits using eq 2 are shown for the pure polyphenylene core of the first generation and for the corresponding poly-Z-L-lysine functionalized PPDs with different polypeptide number of residues (*n* from 14 to 84). The correlation curves are shifted to longer times with increasing poly-Z-L-lysine length. Also increasing the core size for the first- and second-generation dendrimers shifts the correlation curves to longer times (Figure 2, bottom).

The fits to the experimentally measured autocorrelation curves shown in Figure 2 can be used in the evaluation of the diffusion times resulting in diffusion coefficients and hydrodynamic radii of the polyphenylene cores and the respective poly-Z-L-lysine functionalized PPDs. As the observation volume depends strongly on the specific optical setup and cannot be measured directly, suitable calibration procedures have to be devised first. FCS calibration in aqueous environment typically relies on the straightforward measurement of the characteristic diffusion time of a dye molecule with known diffusion coefficient, i.e., rhodamine 6G. In organic media, however, no such simple means is available. Most dye molecules tend to aggregate in organic solvents, and in contrast to aqueous systems the diffusion coefficients are barely known.[20] Therefore, the observation volume was calibrated using fluorescently labeled silica nanoparticles. As the nanoparticles are relatively large

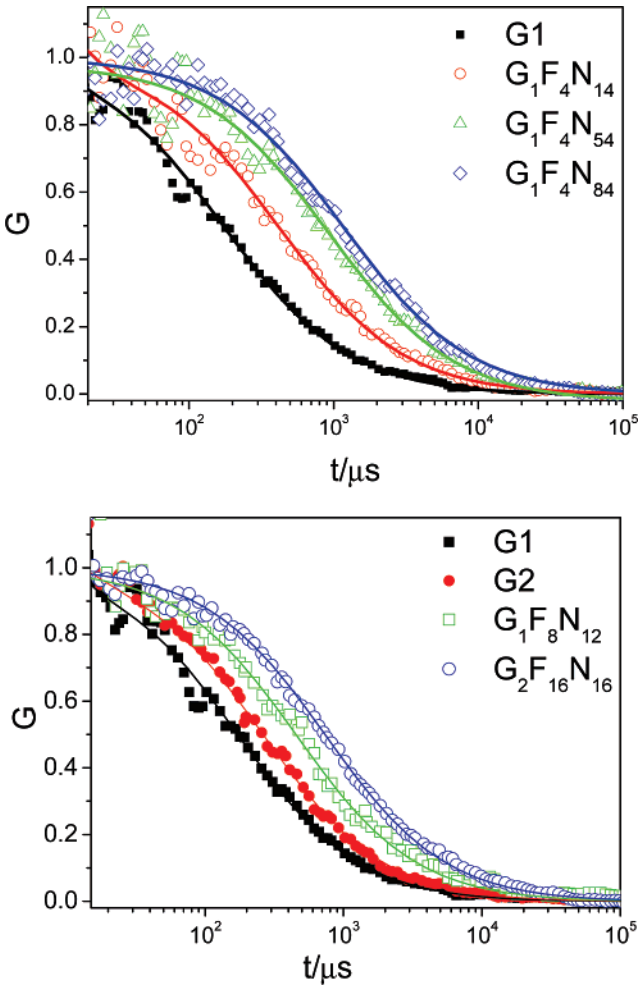

Figure 2. (Top): Effect of increasing the poly-Z-L-lysine length on the correlation curves for the poly-Z-L-lysine functionalized polyphenylene dendrimers (PPDs) of the first generation. Filled squares, pure core of the first generation; circles, $G_1F_4N_{14}$; triangles, $G_1F_4N_{54}$; rhombus, $G_1F_4N_{84}$. (Bottom): Effect of increasing the core size on the correlation curves for the functionalized PPDs with similar poly-Z-L-lysine length. Filled squares, pure core of the first generation; filled circle, pure core of the second generation; squares, $G_1F_8N_{12}$; circles, $G_2F_{16}N_{16}$.

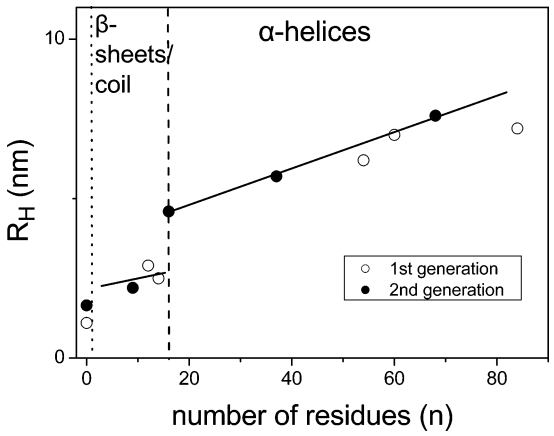

Figure 3. Dependence of the hydrodynamic radius (obtained from the SE equation) on the number of lysine residues in the corona for first- and second-generation poly-Z-L-lysine functionalized polyphenylene dendrimers (PPDs). The dotted and dashed lines separate, respectively, the polyphenylene cores from the coil/β-sheet conformations and from the α-helical poly-Z-L-lysines as detected by ^{13}C NMR spectroscopy. The solid line with a slope of 0.058 nm/residue is a linear fit to the second-generation dendrimers with $n \geq 16$, whereas the line for $n < 16$ is a guide for the eye. The estimated error is approximately twice the symbol size.

their hydrodynamic radius and diffusion coefficient in DMSO solution were easily measured with DLS.

The results on the hydrodynamic radii of the poly-Z-L-lysine substituted PPDs, evaluated using the above FCS calibration procedure and eq 3, are shown in Table 1. The hydrodynamic radii of the pure polyphenylene cores were also measured and found to be 1.1 and 1.7 nm for the first and second generation, respectively. If on the other hand an ellipsoidal shape is assumed (eq 4) for G_1 and G_2, then the length L can be slightly higher than the radii obtained using eq 3. For example, assuming a cylinder of length L and diameter d with an aspect ratio of 3 the calculated effective radius is $L = 1.4$ nm as compared to the 1.1 nm from the spherical model (and this value is closer to the estimated polyphenylene core radius based on modeling). The results for all compounds of Table 1 are summarized in Figure 3, which displays a clear dependence of the obtained hydrodynamic radii on the core and the polypeptide size. More specifically, oligolysine-functionalized PPDs display smaller hydrodynamic radii as compared to their poly-Z-L-lysine counterparts. In particular, an abrupt increase in R_H is observed for $n \geq 16$. In Figure 3, the slope (dR_H/dx) from the second-generation poly-Z-L-lysine functionalized PPDs results in 0.058 nm/residue. We note that this value is lower than the expected 0.15 nm/residue found for polypeptides in their α-helical conformation. We will return to this point later with respect to the NMR results. On the other hand, increasing the poly-Z-L-lysine functionality has a small effect on the hydrodynamic radii (compare for example $G_1F_4N_{14}$ with $n = 14$ with $G_1F_8N_{12}$ with $n = 12$ or $G_1F_4N_{54}$ with $n = 54$ with $G_1F_8N_{60}$ with $n = 60$). In addition, to have an independent estimate of the sizes involved in the diffusion measurements, DOSY experiments were performed for selected examples ($G_2F_8N_{37}$ and $G_2F_{16}N_{68}$) in solutions similarly dilute as those used in FCS. As expected, the results from DOSY confirmed the FCS values reported in Table 1 and as Supporting Information.

In order to explore the origin of the $R_H(n)$ dependence shown in Figure 3 and the abrupt increase of the hydrodynamic radii for $n \geq 16$, we performed ^{13}C solution NMR and FTIR that are sensitive probes of the peptide secondary structures. In the former the different conformations can be distinguished due to the differences in the ^{13}C chemical shifts, arising from variations of the dihedral angles (Φ and Ψ).[21] Thus, ^{13}C solution-state NMR spectroscopy has been employed to differentiate between the α-helical and β-sheet conformations. In the latter, the amide I and II bands at 1655 and 1550 cm^{-1}, respectively, associate with α-helical conformations, whereas the band at 1630 cm^{-1} is the shifted amide I band (amide C═O stretch) component to lower frequencies associated with the β-sheet conformations. From the above experiments and for the dilute concentrations employed herein, only ^{13}C NMR could provide a definite answer with regard to the peptide secondary structure.

In Figure 4, ^{13}C NMR spectra are plotted for some of the solutions studied. For α-helices chemical shifts of 175 and 57 ppm are expected[21] for the amide C═O and the C_α carbon, respectively, which are indeed observed for poly-Z-L-lysines with $n \geq 16$. For shorter peptides with $n = 14$ and $n = 9$, however, chemical shifts at 172 and 53 ppm are detected for these carbons, indicative of β-sheet secondary structures. In comparison to a solution, where the compounds tumble fast—on the NMR time scale—leading to effective averaging of the anisotropic interactions and thus to sharp spectral lines, the resonance peaks of the dendrimers appear broadened. The full

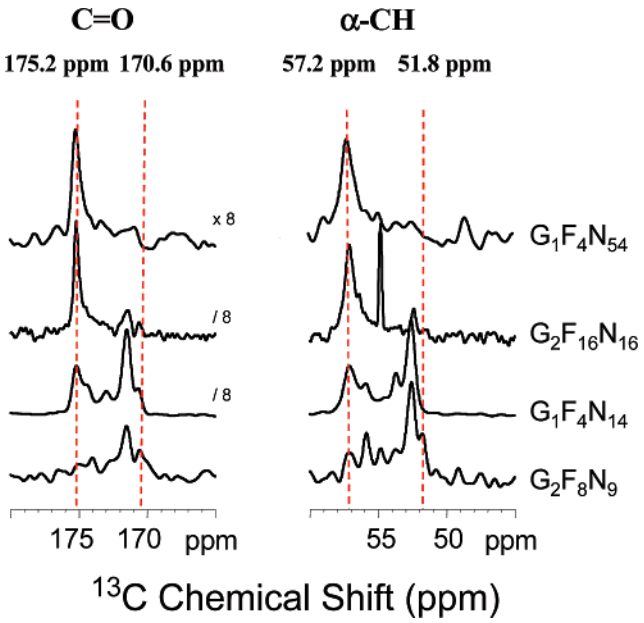

Figure 4. ^{13}C NMR spectra of four poly-Z-L-lysine substituted polyphenylene dendrimers (PPDs) at the C_α and amide C=O resonances taken at 298 K. The vertical lines give the expected chemical shifts for C_α and amide C=O resonances for α-helices and *β*-sheets (ref 20). Notice the change from coil/*β*-sheet conformations to α-helical at $n \geq 16$.

width at half-height of the peaks varies from 75 to 180 Hz with the tendency of being sharper in the amide C=O region of the expected α-helical conformation in dendrimers having a degree of polymerization $n > 16$. The sharp resonance observed at 54.5 ppm in the aliphatic region of the ^{13}C spectrum of $G_2F_{16}N_{16}$ has no counterpart in the amide C=O region. Thus, the peak does not arise from a specific conformation inherent to the sample studied but is most probably due to a dissolved contamination. The broadening of the resonances and the broad features spanning the whole range between 172−175 ppm and 52−55 ppm are most pronounced for $n < 14$ and can originate, in principle, from a distribution of conformations in the peptide chains as well as from aggregation. Here, a comparison of ^1H and ^{13}C NMR is most informative. Aggregation would lead to slowing down of the poly-Z-L-lysine dendrimers and interdigitation of the peptide chains. The reduction of mobility would result in broadening of the ^1H NMR spectra, which is not observed. Moreover, we performed DOSY experiments on the same concentrated solutions used in ^{13}C NMR. Use of the SE equation with the measured solution viscosity (from rheometry) provided no evidence in support of aggregation. Therefore, the broadening of the ^{13}C resonances is ascribed to a distribution of peptide conformations. Notice that, even for the longer poly-Z-L-lysines, the resonances appear somewhat broadened; however, the predominant conformation for $n \geq 16$ is clearly α-helical.

Therefore, the origin of the distinct increase in the hydrodynamic radii for $n \geq 16$ is the change of the peptide secondary structure from coil/*β*-sheet conformations to predominantly α-helical conformations. A similar change of polypeptide conformation was also observed in the bulk,[8] where the α-helical conformation dominates for poly-L-lysine functionalized PPDs with intermediate degrees of polymerization ($16 < n < 37$), while the packing requirements of the chains determine the mixed α-helical/*β*-sheet conformation detected in the longer chain analogues. This change in secondary structure and the consequences on the conjugates diffusion can be crucial in the design of MAPs.

The distribution of different types of the secondary structures for short oligopeptide chains with $n < 14$ deserves a comment. Generally, one can envisage three possibilities for such behavior: (i) local separation of dendrimers with purely α-helical and those with purely *β*-sheet conformations; (ii) coexistence of purely α-helical and purely *β*-sheet conformations in different peptide chains within the same dendrimer; (iii) coexistence of different conformations in the same chain. Local separation (i), however, does not seem likely for thermodynamic reasons. Moreover it would lead to molecules with different hydrodynamic radii in the FCS and DOSY solutions—some with the elongated α-helical conformation and some with the more compact *β*-sheet secondary structure.[22−24] No indication of this was observed in the FCS and DOSY experiments. Coexistence of α-helical and *β*-sheet type conformations in different peptide chains within the same dendrimer (ii) and coexistence of different conformations in the same chain (iii) are difficult to distinguish as both reflect a nonuniform distribution of conformations.

As to the physical reason for the change in peptide conformation, we recall that an interconversion between the two main peptide secondary conformations has been reported before in different polypeptides. The parameters that can initiate such changes include interactions with solvent molecules and method of reprecipitation,[22] temperature,[23] number of residues,[8,21,25] packing ability,[8] and even mechanical force[22] in the solid state. We have shown recently[8] that the packing ability and number of residues were the main factors controlling the melt self-assembly when the same PPDs were functionalized with poly-L-lysine chains. In the present case of dilute solution all parameters remain fixed except for the number of residues. Therefore, the *β*-sheet/α-helix transformation can be attributed here solely to the stabilization of the α-helical conformation due to the increasing poly-Z-L-lysine length.

IV. Conclusions

Fluorescence correlation spectroscopy and diffusion-ordered NMR experiments have been employed to detect the effects of the size, functionality, and peptide secondary structure on the diffusion coefficient and hydrodynamic radius in a series of poly-Z-L-lysine functionalized polyphenylene cores bearing the fluorescent perylenediimide dye in DMSO solutions. This allowed us to determine the size of the molecules at very dilute concentrations. In parallel, ^{13}C NMR has been employed to follow the peptide secondary structure in DMSO solutions. We found that the change in the peptide secondary structure from coil/*β*-sheet conformations to α-helices detected by ^{13}C NMR spectroscopy is accompanied by an abrupt increase in the hydrodynamic radii. It has been shown that FCS is a sensitive probe of the core size and of the change in peptide secondary structure but less sensitive to functionality.

Acknowledgment. Financial support by the DFG (SFB 625) and by the Greek GSRT (PENED 529 and 856) is gratefully acknowledged.

Supporting Information Available. ^1H NMR DOSY spectra of the dilute $G_2F_8N_{37}$ and $G_2F_{16}N_{68}$. This material is available free of charge via the Internet at http://pubs.acs.org.

References and Notes

(1) Wiesler, U.-M.; Weil, T.; Müllen, K. *Top. Curr. Chem.* **2001**, *212*, 1.
(2) Stiriba, S.-E.; Frey, H.; Haag, R. *Angew. Chem., Int. Ed.* **2002**, *41*, 1329.
(3) Veprek, P.; Jezek, J. *J. Pept. Sci.* **1999**, *5*, 203.
(4) Tam, J. P. *J. Immunol. Methods* **1996**, *196*, 17.
(5) Tam, J. P.; Lu, Y.-A.; Yang, J.-L. *Eur. J. Biochem.* **2002**, *269*, 923.
(6) Tam, J. P.; Lu, Y.-A. *Proc. Natl. Acad. Sci. U.S.A.* **1989**, *86*, 9084.
(7) Mihov, G.; Grebel-Koehler, D.; Lübbert, A.; Vandermeulen, G. W. M.; Herrmann, A.; Klok, H.-A.; Müllen, K. *Bioconjugate Chem.* **2005**, *16*, 283.
(8) Mondeshki, M.; Mihov, G.; Graf, R.; Spiess, H. W.; Müllen, K.; Papadopoulos, P.; Gitsas, A.; Floudas, G. *Macromolecules* **2006**, *39*, 9605.
(9) Eigen, M.; Rigler, R. *Physica A* **1994**, *91*, 5740.
(10) Rigler, R.; Grasselli, P.; Ehrenberg, M. *Phys. Scr.* **1979**, *19*, 486.
(11) Walter, N. G.; Schwille, P.; Eigen, M. *Proc. Natl. Acad. Sci. U.S.A.* **1996**, *93*, 12805.
(12) Magde, D.; Elson, E.; Webb, W. W. *Phys. Rev. Lett.* **1972**, *29*, 705.
(13) Cluzel, P.; Surette, M.; Leibler, S. *Science* **2000**, *287*, 1652.
(14) Morris, K. F.; Cutak, B. J.; Dixon, A. M.; Larive, C. K. *Anal. Chem.* **1999**, *71*, 5315.
(15) Grimsdale, A.; Muellen, K. *Angew. Chem., Int. Ed.* **2005**, *44*, 5592−5629.
(16) Jang, Y.-J.; Atanasov, V.; Klapper, M.; Müllen, K. Unpublished results (2006).
(17) Johnson, C. S. *Prog. Nucl. Magn. Reson. Spectrosc.* **1999**, *34*, 203−256.
(18) Haustin, E.; Schwille, P. *Curr. Opin. Struct. Biol.* **2004**, *14*, 531.
(19) Tirado, M. M.; Garcia de la Torre, J. *J. Chem. Phys.* **1980**, *73*, 1986.
(20) Zettl, H.; Haefner, W.; Bo1ker, A.; Schmalz, H.; Lanzendorfer, M.; Mueller, A. H. E.; Krausch, G. *Macromolecules* **2004**, *37*, 1917.
(21) Shoji, A.; Ozaki, T.; Saito, H.; Tabeta, R.; Ando, I. *Macromolecules* **1984**, *17*, 1472.
(22) Henzler Wildman, K. A.; Lee, D. K.; Ramamoorthy, A. *Biopolymers* **2002**, *64*, 246.
(23) Lee, D. K.; Ramamoorthy, A. *J. Phys. Chem*. **1999**, *B103*, 271.
(24) Henzler Wildman, K. A.; Wilson, E. E.; Lee, D. K.; Ramamoorthy, A. *Solid State Nucl. Magn. Reson.* **2003**, *24*, 94.
(25) Papadopoulos, P.; Floudas, G.; Klok, H.-A.; Schnell, I.; Pakula, T. *Biomacromolecules* **2004**, *5*, 81.

BM0702760